

# POTENTIOMETRIC DETECTION OF AMMONIUM ION IN SOIL SAMPLES OF ROHTAK BY DEPOSITION OF UREASE NANOPARTICLES ONTO PTFE MEMBRANE ON AMMONIUM ION SELECTIVE ELECTRODE

BINDU<sup>1</sup>, NAVEENA DINODIA<sup>2</sup>, VIKAS ABROL\* AND SEEMA KUMARI\*

Department of Botany, Baba Mastnath University, Rohtak, Haryana, India

(Received 20 September, 2023; Accepted 7 November, 2023)

**Key words:** Soil, Ammonia, Biosensor, AISE, Urease, PTFE, FESEM, Nanoparticles, FTIR.

**Abstract**– The present study focuses on the urease nanoparticles preparation by desolvation method functionalized by cysteamine dihydrochloride and characterization of UrsNPs potentiometric biosensor for detecting ammonium ions level in soil. The biosensor was prepared by immobilizing these nanoparticles onto an activated PTFE membrane and bounded it with an ammonium ion selective electrode (AISE). Characterization of UrsNPs and immobilization onto PTFE membrane was done by Fourier transform infrared spectroscopy (FTIR) and field emission scanning electron microscopy (FESEM) techniques, which reveals nanoparticle diameters ranging from 13nm to 90nm. The ENPs were more active and stable with a longer shelf life than native enzyme molecules. The ENPs were immobilized onto chitosan (CHIT) activated PTFE membrane via glutaraldehyde coupling with 86.71% retention of initial activity of free urease NPs with a conjugation yield of 1.64 mg/cm<sup>2</sup>. This membrane was mounted at the lower end of the ammonium ion selective electrode (AISE) with O-ring and then electrode was connected to a digital pH meter to construct a potentiometric urea biosensor. The biosensor exhibited optimum response within 10 s at pH 5.5 and 40 °C. The biosensor exhibited potentiometric responses of NH<sub>4</sub><sup>+</sup> in soil samples with linear detection range of concentration between 0.01-0.80mM, low detection limit of 0.005mM respectively and sensitivity rate with a slope of 38mV/decade. Analysis of the additional urea revealed that the following percentages were recovered 107.4%. Due to very negligible amount of urea present in the aqueous solution of soil, the values did not changed and exhibited nearly 0.9830 % coefficient of variation for both with and within the samples. The maximum concentration of ammonium ion in the soil of village Ningana, 0.009ppm. Furthermore, the biosensor's application enabled a comprehensive assessment of ammonium ion levels in diverse communities. The within and between-batch coefficient of variations (CVs) of present biosensor were 0.18% and 0.32% respectively. The biosensor had negligible interference from Cu<sup>2+</sup>, Ag<sup>+</sup>, Ni<sup>+</sup> and Hg<sup>+</sup> had slight interference, which was overcome by specific ion selective electrode. The ENPs bound NC membrane was used maximally 8–9 times per day over a period of 180 days, when stored in 0.01M sodium acetate buffer pH 5.5 at 4 °C.

## INTRODUCTION

Today, urea, or nitrogen, is the most widely used nitrogenous fertiliser, being utilised in around 46% of all agricultural worldwide. Conventional chemical fertilisers are the most frequently used fertilisers worldwide in order to enhance production in agricultural systems and provide enough food for the growing global population (UN DESA/POP for 2021). Coated urea fertilisers increase nitrogen supply while reducing nitrogen losses from leaching, volatilization, and N<sub>2</sub>O

emission, according to Wei *et al.* (2020). The NUE of nutrient-coated urea was 30–60% lower than coated urea, making it more efficient (Chen *et al.*, 2020). Coating increases urea uptake and yield generation by using 20–30% less urea than would otherwise be required. According to Zhu *et al.* (2020), it increases 23.4% nitrogen agronomy efficiency (NAE), decreases 34.65% nitrogen fertilizer utilization rate, and improves 25.83% nitrogen physiological efficiency (NPE). Fertilizers made of granulated urea is applied to the soil or dissolved in irrigation water. Urea alters the chemical, physical, and transport

properties of soil.

Some microbes convert urea into ammonia ( $\text{NH}_4^+$ ). Microorganisms turned ammonium into nitrate ( $\text{NO}_3^-$ ) and nitrate into gaseous nitrogen oxides and molecular nitrogen when anaerobic conditions were present (LV *et al.*, 2024). Urease hydrolyzed urea N at 37 °C in soil at a rate of 2.48 to 15.91g per gram per hour (Gupta, *et al.*, 1992). Herbivorous animals urea serves as a source of nitrogen for plants. Chemical processes are brought on by the conversion of nitrogen from plants and animals to organic molecules and subsequent urea regeneration. The urea solution reduced the soil's capacity to hold water. As urea solution concentration increased, so did the size of soil macropores. When urea solution was applied, the quantity of mesopores and micropores in the soil decreased (ZJ *et al.*, 2023). Urea makes up 73.4% of all N fertilizer used globally, making it a significant source of N due to its significant influence on crop yield across borders 2019 and (Dubowski, Kira, Shaviv).

The state of Haryana (India), one of the most agriculturally productive areas in the country, is important from an agro ecological stand point. The demand for sensitive and precise urea measurement techniques in many matrices, including milk, soil extracts, seawater, and wine, is growing (Lambert *et al.*, 1992). For the sake of product quality and regulatory compliance, the urea content of urea-based fertilizers needs to be precisely determined. This is especially true for fertilizers whose urea concentration has undergone physical or chemical modification. Free (unreacted) urea cannot be regarded as a part of the delayed or controlled-release nitrogen component because it is a rapidly accessible nitrogen source and is included in the majority of these fertilizer formulations.

Various methods, such as colorimetric determination of urea in soils and spectrophotometric determination of urea, have been used in the past to measure urea in soil. A high-performance liquid chromatography method with UV detection is used to separate urea and its impurities, such as bi uret, cyanuric acid, and triuret (Hammimed *et al.*, 2023). Specificity, linearity,

correctness, identification, precision, and robustness were the characteristics that were assessed for urea and biuret (Woldemariam *et al.*, 2020). In the current study, a potentiometric method is used to calculate the ammonium content of soil. Nature contains large amounts of the molecule urea, and research on this substance is crucial for agricultural chemistry, food science, environmental monitoring, and medical care (Pundir *et al.*, 2018, Chauhan and Thakur., 2023). With a molecular weight of 60g/mol, urea is a tiny, two-atom, water-soluble byproduct of the metabolism of nitrogen and proteins (Raymond *et al.*, 2018). It is a tasteless, colourless solid that dissolves easily in water and has essentially no harmful effects (Wei *et al.*, 2001; Dhawan *et al.*, 2009). It has neither acidic nor alkaline qualities.

By converting urea to ammonia ( $\text{NH}_3$ ), carbonic acid ( $\text{H}_2\text{CO}_3$ ), and carbamic acid ( $\text{H}_2\text{NCOOH}$ ) via carbamic acid, a nickel enzyme known as urease (EC 3.5.1.5) breaks down urea (Fig.1).1. In aqueous solutions, bicarbonate ( $\text{HCO}_3^-$ ) and ammonium ( $\text{NH}_4^+$ ) ions balance the concentrations of carbonic acid and  $\text{NH}_3$  in turn. Invertebrates, fungi, bacteria, and plants all generate urease, and the majority of these species share a great deal of structural and functional similarities. Two  $\text{Ni}_{2+}$  ions are connected via a carbamylated lysine and hydroxyl group in the urease active site (Savane *et al.*, 2020).

For assessing the physiological condition of important electrolytes, potentiometry using polymeric membrane ion-selective electrodes (ISEs) is a well-established analytical technique. Potentiometric sensors provide a number of benefits, including small size, quick response time, simplicity of use, low cost, and resistance to turbid and coloured interferences. ISEs have a variety of additional distinguishing characteristics. They offer data on the concentration of free ions (ion activity), as opposed to other analytical procedures that produce total concentration. The detection limits are, at least theoretically, independent of sample volume and are unaffected by a considerable reduction in sample volume. These characteristics, according to Jiawang and Wei (2020), distinguish ISEs as an indication electrode or detector. Academics from a variety of fields are interested in

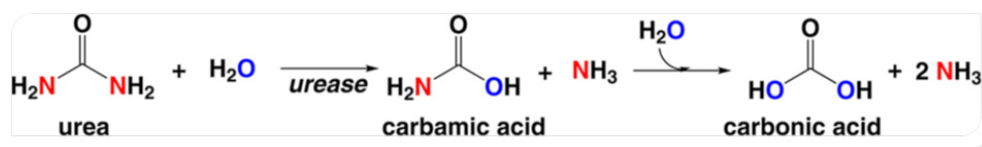


Fig. 1. Schematic breakdown of urea by urease in its byproducts

ammonium ion concentration since it is a crucial indicator for environmental and medical applications. As an example, ammonium is thought to be both a possible biomarker of an enzyme by product in significant physiological reactions and a naturally occurring indicator of water quality. Due to benefits like cost effectiveness, user friendliness, and miniaturisation ability, which enables simple portable measurements, potentiometric ion-selective electrodes (ISEs) have attracted the attention of the scientific community as an alternative to conventional analytical methods used to detect ammonium ions (Cuartero *et al.*, 2020). For efficient fertiliser management in plant growth and monitoring nitrogen cycle dynamics, accurate determination of  $\text{NH}_4^+$  levels in soil samples is essential. For this reason, conventional techniques including liquid chromatography (IC), flow injection analysis (FIA), and colorimetric tests are frequently used. However, these methods have drawbacks, such as high costs and complexity, which restrict their use to farmers. Farmers frequently view colorimetric assays offered for field use as difficult and pricey. Therefore, a sensitive, easy-to-use, and affordable technique for  $\text{NH}_4^+$  detection in soil samples is urgently needed, especially for usage in agricultural contexts. We have created a potentiometric biosensor with urease enzyme immobilised on a PTFE membrane for soil ammonia detection and measurement in order to overcome these difficulties.

## METHODOLOGY

**Materials used:** Urease, sodium phosphate buffer, tris-acetate buffer, ethanol, DSS, cyst amine dihydrochloride, chitosan, methanol, deionized water, ISAB (Internal Standard Addition Buffer), 25% DSS solution (for the preparation of 2.5% DSS), Nessler's reagent, tri-chloroacetic acid (TCA), and absolute ethanol are among the reagents needed for the procedures.

**Instruments used:** Digital ion meter, Water bath,, Sonicator, UV spectrophotometer, Weighing balance, Magnetic stirrer, Centrifuge, Ammonium ion selective electrode:, FTIR, FESEM.

### Assay of free Urease enzyme

A standard curve of  $\text{NH}_4^+$  concentration vs. absorbance at 405 nm was used to extrapolate the concentration of  $\text{NH}_4^+$  produced throughout the experiment. The amount of enzyme required to release 1 mol of ammonia from the hydrolysis of urea in 1 minute under standard test conditions was found to be equal to one unit of enzyme activity.

**Preparation of urease nanoparticles and immobilization:** The already-isolated Urease enzyme was bought from SIGMA ALDRICH. The method described by Jakhar *et al.* (2018) was used to produce and immobilise the nanoparticles onto PTFE membrane.

**Characterization of free urease nanoparticles:** The produced urease nanoparticles sizes were determined using FTIR and FESEM studies.

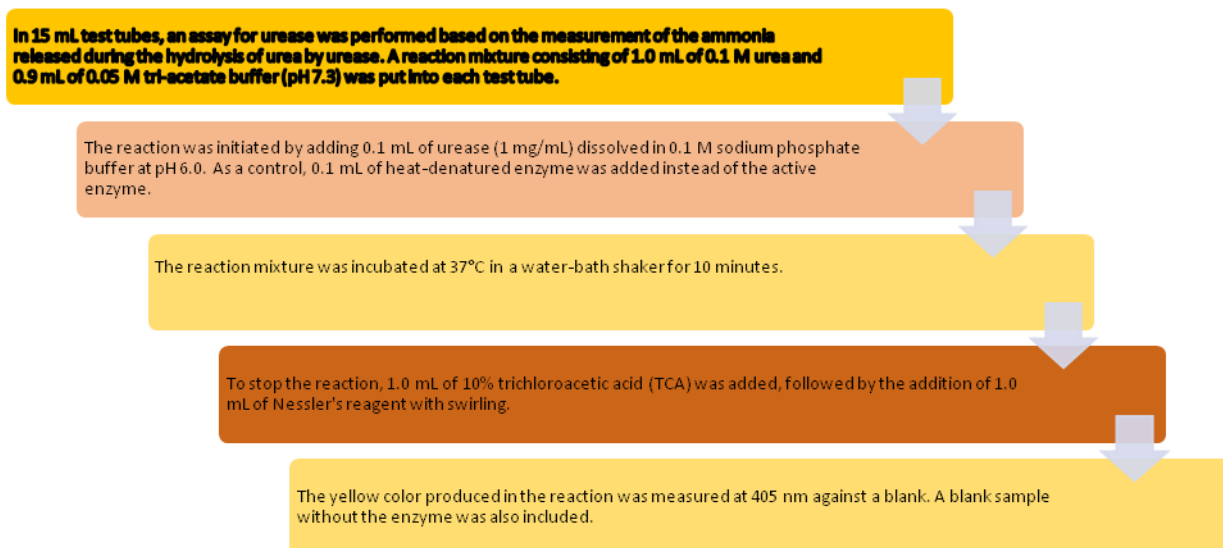
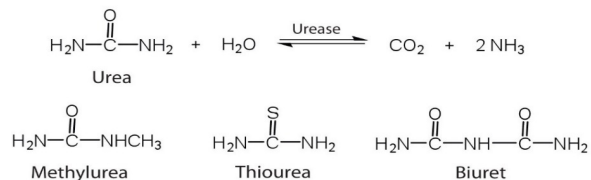


Fig. 2. Stepwise representation of enzyme assay.

**Characterization of urease immobilized PTFE membrane:** FESEM images of the membrane were taken both before and after urease immobilisation in order to verify its success.

**Preparation of AISE electrode:** Labman supplied the Ammonium Ion Selective Electrode (AISE). It was calibrated by dipping it in a 10% KCl solution for 30 minutes, then calibrating for constant readings, as instructed in the electrode handbook.



**Optimization of Potentiometric Urea biosensor:** According to the method recommended by Jakhar and Pundir in their 2017 study, the prepared urea biosensor was optimised for pH, temperature, effect of substrate concentration, response time, linear range, detection limit, analytical recovery, sensitivity, precision, reproducibility, storage stability, and interference of some metabolites.

**Analysis of NH<sub>4</sub><sup>+</sup> in soil using ISEs**

**Study sites and sampling** The study area is Kalanaur, which is located in Haryana’s Rohtak District. The research area is Kalanaur Block of Rohtak District, which is located in Rohtak’s southern region in the state of Haryana. It is surrounded by the districts of Rohtak city in the north and east, Jhajjar in the south east, Bhiwani in the west, Charkhi Dadri in the south west, and Kalanaur, which is about 22.5 kilometres from Rohtak city. Chandigarh, the capital of Haryana, is 292 kilometres and 85 km, respectively, away from Kalanaur. Its coordinates are 28° 49' 39.108" latitude and 76° 23' 41.352" longitude. It is 200 metres (700 feet) above sea level on average. The Kalanaur’s temperature ranges from 3 °C to 44 °C. Rainfall is the annual amount of precipitation, primarily in the month of (200-240mm).The summer and winter temperatures are extremely high due to the semi-arid climate. 8.7 °C to 20.7 °C in the winter and 35 °C to 45 °C in the summer. 18% relative humidity is the average. Dec. to Feb. is the winter season.

All 26 villages in the Kalanaur Block of the Haryana district of Rohtak were included in the research area. In these villages, soil samples were collected in the month of March of this year. Surface

10-15 cm (top soil) soil samples would be taken from various parts of Kalanaur Block, Rohtak district. For examination, soil samples were sieved to a thickness of 4mm, stored in airtight polythene jars, and kept at 4 °C for a maximum of one week. 100 cc of distilled water was used to log 20 g of dirt before it was filtered. The water that had been percolating was collected, and its ammonium content was checked.

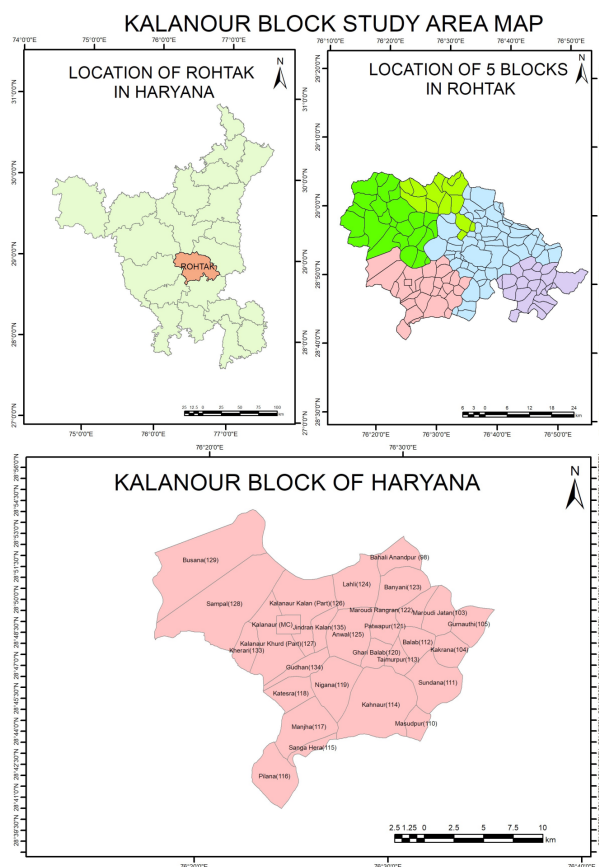


Fig. 3. Geotag map of Kalanaur blocks

**Background soil analysis:** For the examination of several soil qualities, such as pH, phosphorus, potash, and nitrogen, soil samples that had been sieved were employed. Both the soil kit method and the ion metre were used to determine the pH of the soil sample. The soil kit method was used to measure phosphorus, potash, and nitrogen.

Table 1. Values achieved by background soil analysis

Soil properties	Lowest value	Highest value
pH	5.6	8.4
Nitrogen	<140	280-560
Phosphorous	5-10	>40
Potash	< 100	280-560
Organic Carbon	< 0.25	1.1-1.3



**Extraction procedure of  $\text{NH}_4^+$  from soil:** A 100 ml beaker is filled with about 20g of dried soil. The 80ml of distilled water is then added to the beaker. A magnetic stirrer was used to mix the sample for 10 minutes before being centrifuged at 5000 rpm for 30 min. The suspension was then filtered using Whatman filtered paper, and the sample was used for analysis.

**Analysis of  $\text{NH}_4^+$  in soil samples using AISE:** The ammonia emitted from the samples was measured using a Lab man Ammonium Ion Selective Electrode (AISE). An electrical connection was made between the electrode and a Lab man digital ion metre, which displayed ammonia, pH, and potential values. To release ammonia, each sample was put through a TISAB with a Lab man electrode. Simply mix the soil with 80 ml of water, filter the mixture through Whatmann's filter paper, and then add 20 ml of this aqueous soil solution to the electrode. 1 cc of TISAB was added to help release the bound ammonium ions.

## RESULTS AND DISCUSSION

**Enzyme assay** UV-visible absorption spectroscopy revealed considerable structural changes caused by urease NP production in NP aggregates. The dramatic fluctuations in absorbance peaks and the improved absorbance within the aggregates allowed for the efficient synthesis of urease NP aggregates while preserving the enzyme's characteristic molecular structure.

**Preparation of urease nano-particles:** In order to produce urease nanoparticles (NPs), ethanol desolvation was used at 4 °C. Stable urease-NP aggregates were created by decreasing the hydration

layer that surrounds urease molecules and boosting interactions such as Vander Waals, hydrophobic, and electrostatic forces. We cross-linked the aggregates using glutaraldehyde, which cooperated with the  $-\text{NH}_2$  groups added by cysteamine dihydrochloride to ensure their long-term stability and enzymatic activity. These urease-NP aggregates dramatically higher enzymatic activity was most likely caused by increased active site exposure and possible structural changes during the aggregation process.

**Characterization of urease nano-particles:** The size and shape of urease NP aggregates were investigated using FESEM, as shown in Figure 4a. The urease NPs had an average diameter of 223 nm and a diameter range of 90 to 490 nm. In contrast,

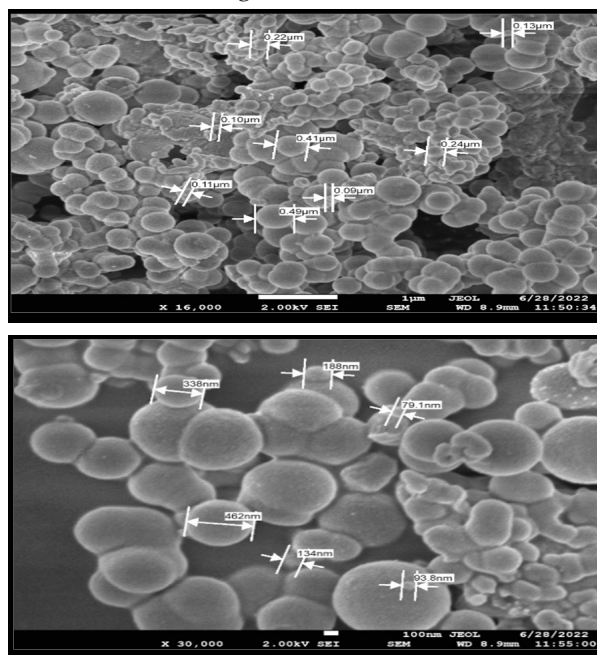


Fig. 4b. FESEM image of urease nanoparticles

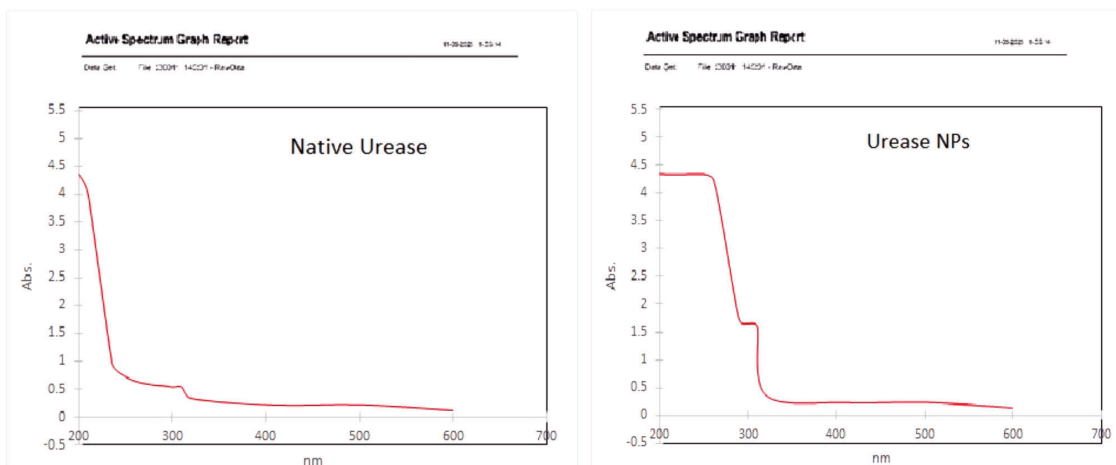


Fig. 4a. Spectrophotometric graph indicating enzyme activity

Turbett *et al.*, 1992 study using TEM measurements of native monomeric urease found a diameter of 13 nm. This finding suggests that each spherical urease NP was created by the aggregated formation of 14 to 18 native urease molecules.

By desolvating urease with ethanol at 4 °C, urease nanoparticles (NPs) were produced. A decrease in the moisture barrier around the urease molecules led to the formation of aggregates by allowing interactions such as Vander Waals forces, hydrophobic forces, and electrostatic forces to occur. The aggregates were nearly permanently cross-linked with glutaraldehyde while keeping their structural integrity and enzymatic activity thanks to the -NH<sub>2</sub> groups from cysteamine dihydrochloride. According to the urease-NP aggregates' markedly increased enzymatic activity, which was most likely caused by increased active site exposure and potential structural changes during aggregation.

The curves observed at different wavelengths indicated different bond stretching which are in similar trend as reported by Jakhar and Pundir in their paper in 2017. In Fig. 3C, curve 1 from 4000 to 500 cm<sup>-1</sup> wave numbers shows FTIR spectra for native urease, while curve 2 shows the spectra for urease NPs aggregates. The FTIR spectra of urease and urease-NPs showed the stretching vibration bands at transmittance (3433.1, 3433.2 cm<sup>-1</sup>) with -NH and -OH stretching due to cysteamine dihydrochloride, (2067.51, 2076.62 cm<sup>-1</sup>) with N-H and C<sup>^</sup>N stretching, (1637.12, 1637.23 cm<sup>-1</sup>) with

C<sup>^</sup>C stretching due to presence of glutaraldehyde, (1164.55, 1167.65 cm<sup>-1</sup>) with C-N stretching, (1078.53, 1079.61 cm<sup>-1</sup>) with C-O stretching, (936.58, 937.67 cm<sup>-1</sup>) with =C-H bending, (670.34, 685.48 cm<sup>-1</sup>) with C-H and C-C bending respectively. An extra peak at 989.67 cm<sup>-1</sup> appeared in urease NPs, which may be due to C-O stretching.

#### Characterization of PTFE membrane by FESEM

The untreated PTFE membrane's scanning electron microscopy (FESEM) pictures revealed a typical hollow beaded structure. On the other hand, clusters of these nanoparticles in bead-like patterns covered the PTFE membrane's surface after being coated with aggregated urease nanoparticles. This finding demonstrates that urease-NP aggregates are immobilised on the PTFE membrane and are attached to it.

The enzyme was able to maintain 86.71% of its initial activity thanks to this immobilisation technique, which was on par with native enzyme activity. In addition, the conjugation process produced a density of 1.64 mg/cm<sup>2</sup>. This information implies that the urease nanoparticles' covalent immobilisation onto the PTFE membrane improved enzyme activity. Using glutaraldehyde coupling, which linked the amino groups of cysteamine-dihydrochloride and enabled the urease enzyme nps to work on the CHIT-decorated PTFE membrane, made immobilisation easier?

**Construction of potentiometric urea biosensor** The urea-detection potentiometric biosensor was

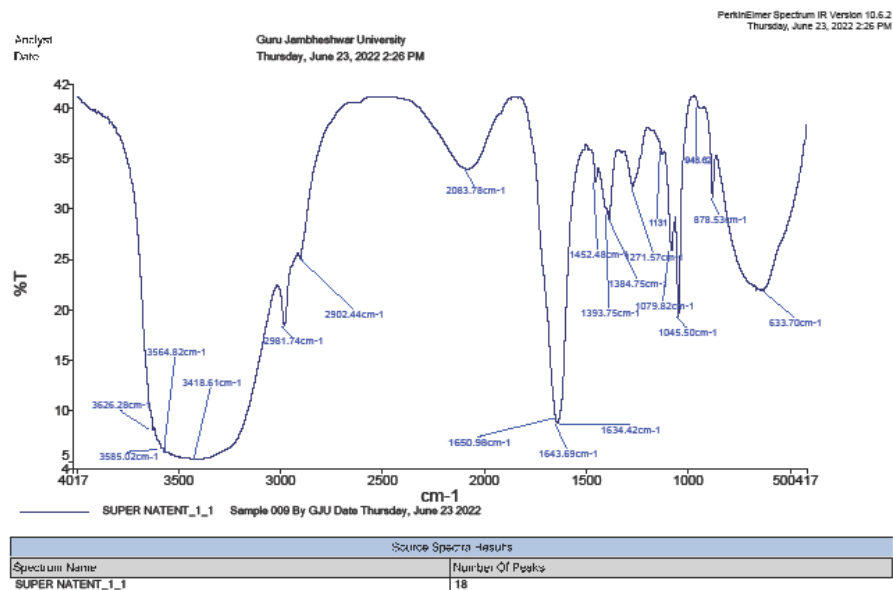
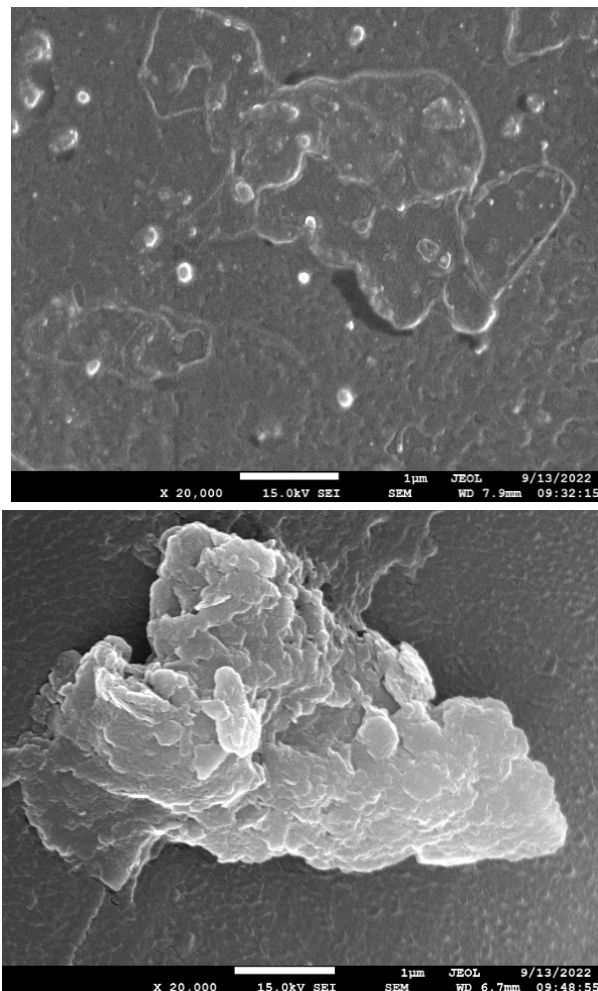


Fig. 5. FTIR graphs of urease nanoparticles



**Fig. 6.** FESEM images of PTFE membrane before and after immobilization of urease nanoparticles

constructed using an ammonium ion selective electrode (AISE) and a PTFE membrane bound with urease nanoparticle (NPs) aggregates. The PTFE membrane containing the aggregate of urease NPs was connected to the lower, more sensitive section of the AISE in this biosensor configuration. Then, this integrated setup was coupled to a digital ion metre.

The potentiometric response was based on the features of the AISE. The simplicity of usage, short response time, non-destructive analysis, broad linear range with adequate selectivity, and extensive use in measuring numerous ions are only a few advantages of this method. In this case, the variable  $\text{NH}_4^+$  concentration in the reaction buffer causes a potential difference to form over time. The potential is altered by the urease's enzymatic decomposition of urea on the NC membrane, which results in  $\text{NH}_4^+$

and  $\text{HCO}_3^-$ . An ammonium ion selective electrode ( $\text{NH}_4^+$  selective electrode) was used to measure this potential shift.

The optimal temperature range for incubating the urease enzyme was discovered to be 35 to 45°C, with 40°C showing the highest activity, 25°C, which is higher than the current temperature, is the optimal temperature for the native urease enzyme to function. The greater thermostability of the engineered nanoparticle (ENP) aggregates may be due to the urease enzyme's higher optimal temperature. There is an improvement in stability due to the aggregation and crosslinking of the enzyme molecules with ENPs, which produces a more stable environment for the enzyme to function efficiently at high temperatures.

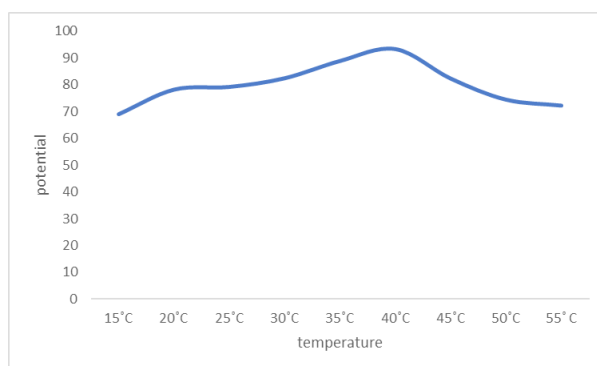


**Fig. 7.** Influence of pH on the potential response of urea biosensor based on urease NPs/PTFE membrane

In contrast to free urease, which functions optimally at a pH of 7.0, the biosensor based on immobilised urease NP aggregates demonstrated its maximum response at a pH of 5.5. This shift in preference for lower pH for maximum activity may be brought on by a potential reduction in the availability of  $-\text{NH}_2$  functional groups within the structure of the enzyme.

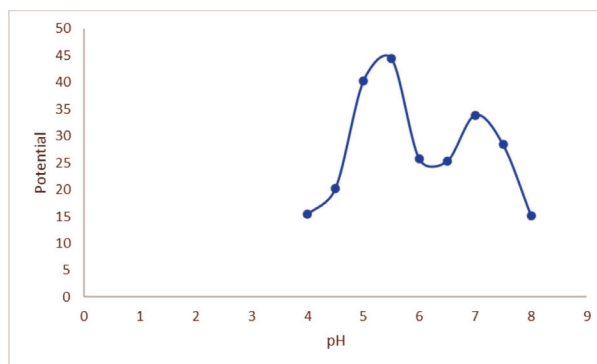


**Fig. 8.** Influence of pH on the potential response of urea biosensor based on urease NPs/PTFE membrane

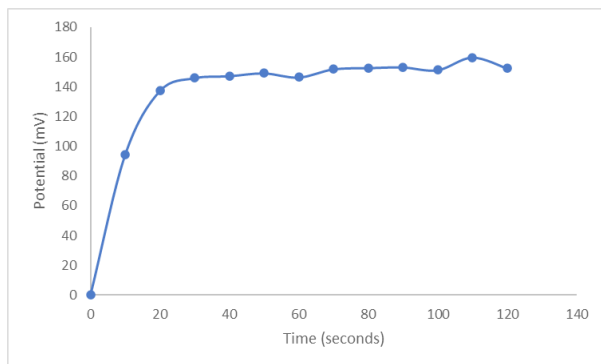


Fig. 9. Voltage vs. Time graph for optimization of response time

Between 10 and 120 seconds, the biosensor’s response time was measured every 10 seconds. It was found that the investigation’s reaction time was comparable to that of other potentiometric urea biosensors that had previously been revealed. It was discovered that there was a hyperbolic relationship between the biosensor’s response and urea concentration, with a range of 1 to 0.25mM. The response was constantly steady above 0.05 mM.

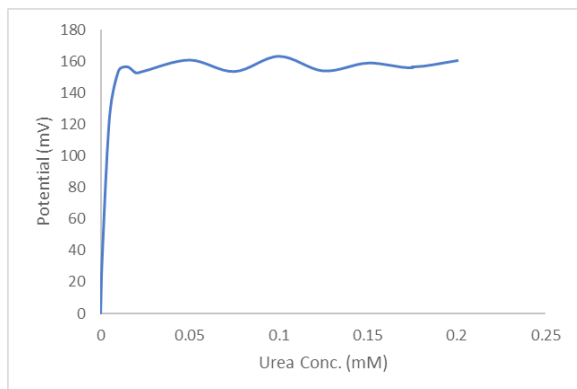


Fig. 10. Voltage vs. Urea graph for optimization of linear range.

Notably, the present urea biosensor’s operating range was expanded from 0.001 to 0.08 mM. Comparing this range to earlier potentiometric urea biosensors, a significant improvement is evident.

**Lower detection limit**

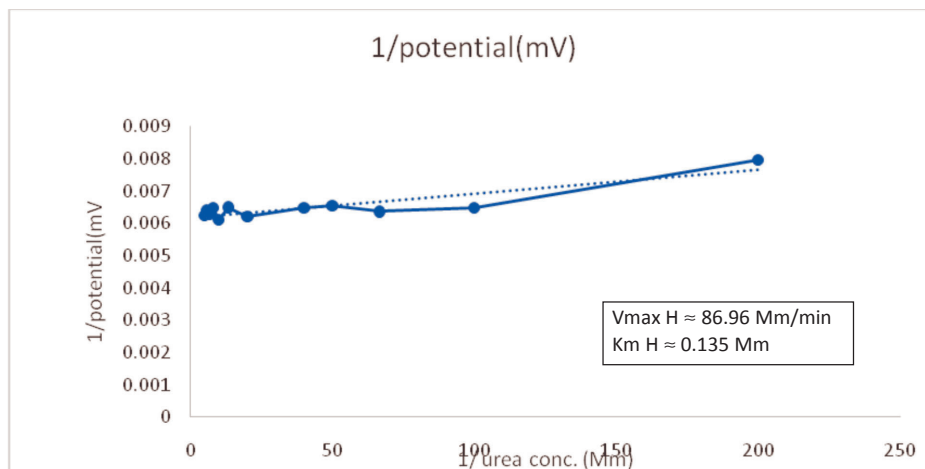
The finding that the novel biosensor’s detection limit is 1 mol/L demonstrates its excellent sensitivity in estimating urea contents. This detection limit is significantly lower than that of numerous other potentiometric urea biosensors based on different matrices that have previously been published, as shown in the Table 1. It’s also crucial to remember that the detection limit of the current biosensor is higher than that of comparison methods, such as the enzymic colorimetric approach, which has a detection limit of 0.0005 M. These findings show the biosensor’s extraordinary potential for very accurate and sensitive urea monitoring..

**Sensitivity**

With a sensitivity of 38mV/decade, the current improved urea biosensor outperforms previously published potentiometric urea biosensors based on diverse materials and techniques.

**Precision**

The within and between-batch coefficient of variations (CVs) of present biosensor were 0.18% and 0.32% respectively for the detection of urea in soil, both within and between samples respectively, when tests were conducted on the same day and after one week of storage at -20 °C. Analysis of the additional urea revealed that the following percentages were recovered 107.4%. Due to very negligible amount of urea present in the aqueous solution of soil, the values did not changed and

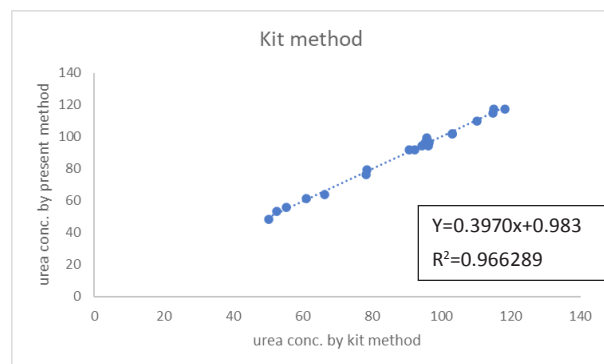




exhibited nearly 0.9830 % coefficient of variation for both with and within the samples. As a result of the biosensor's ability to measure incredibly low urea concentrations with a minimum amount of variance, these results demonstrate the current biosensor approach's excellent repeatability and consistency. A higher urea concentration, however, might result in variations.

### Correlation

The amounts of urea in soil samples were measured using both the reference method and the most recent biosensor technology. On the values obtained using the two methods, a correlation analysis was done using a regression equation. A regression diagram was made to show the relationship between the results of the two methods. The correlation coefficient (CV), which was calculated, was found to have a value of 0.9830. A correlation coefficient that is close to 1 indicates that there is a significant positive correlation between the urea readings provided by the reference method and the current biosensor. This shows that the outcomes produced by the new biosensor technique and the reference technique are comparable. The new biosensing methodology offers a number of advantages over the reference method. These advantages include being quicker, more sensitive, simpler, and more precise. This shows that the novel biosensor approach is more sensitive to urea detection, quicker to provide findings, and simpler to use when compared to the reference method.



### Storage Stability and Reusability of Enzyme Electrode

(Urease- NPs/PTFE/NH<sup>4+</sup> electrode)

The enhanced measuring response of the urea biosensor demonstrated an extraordinary repeatability of 96% for the first 8 to 9 usages. The membrane's efficiency was saturated after this point,

necessitating a step of washing with distilled water. Following this rejuvenation process, which required 4 to 5 hours of rest, the membrane may be used once more. 180 days Later, the enzyme-bound nanoparticle-coated PTFE membrane (ENPs) was still functional. The 0.01M sodium acetate buffer with a pH of 5.5 and a temperature of 4°C was used to maintain the ENPs-bound membrane's functionality for a protracted period of time. Additionally, when stored in distilled water at room temperature, the ammonium ion selective electrode (AISE) showed a 6-month shelf life. The utilisation of cross-linked urease nanoparticle aggregates allowed the immobilised urease system to have a longer shelf life.

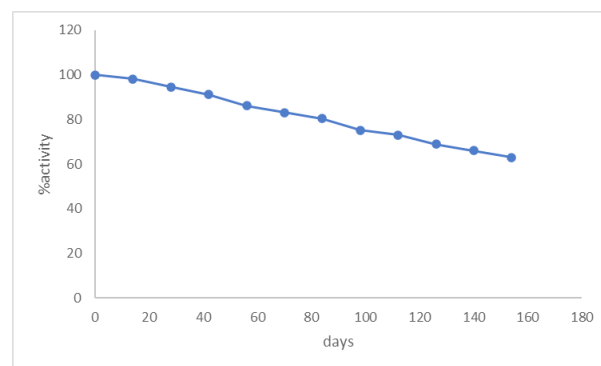
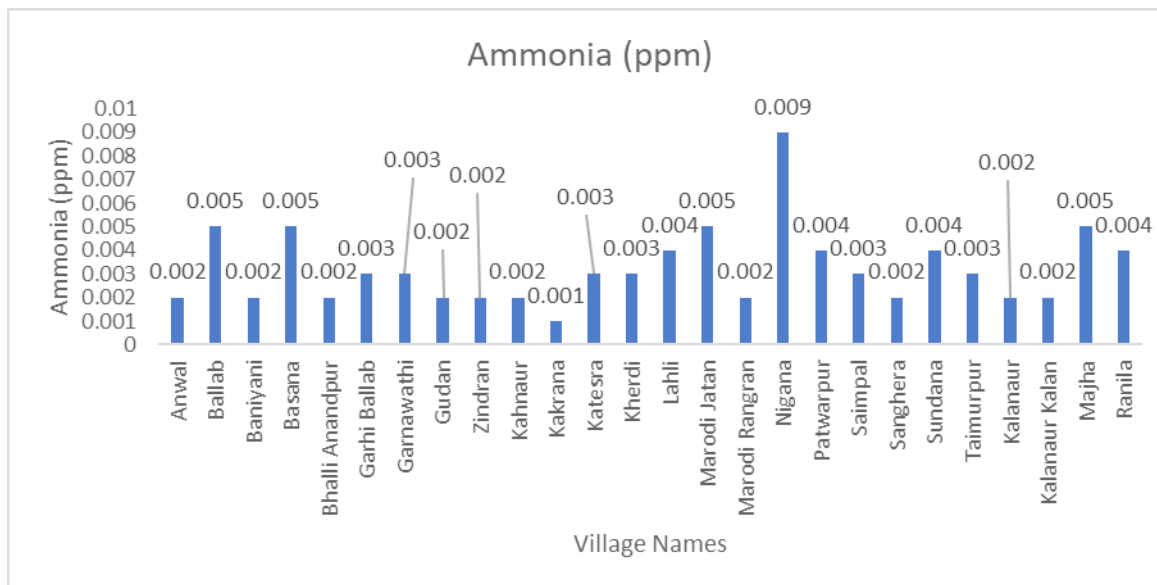


**Table.** Effect of Interfering Substances

Sr. No1	Metal	Inhibition (%)
1	Cu	2.46
2	Ag	22.4
3	Ni	5.96
4	Hg	9.18

Selectivity was determined by using separate solution methods in 0.1M of NaCl solution then electrode response was determined for each interfering ions separately. Each was tested at its physiological concentration to look into how different frequently occurring cations and their associated metabolites affected the biosensor's response. Urea was consistently present in the reaction solution utilised in these interference studies at a concentration of 1.0mM. It is remarkable that the presence of the ions Cu<sup>+</sup>, Ag<sup>+</sup>, Ni<sup>2+</sup>, and Hg<sup>2+</sup> had little effect on the biosensor. Thus, these metabolic ions are defeated by the current ion selective electrode. However, there was some interference when Ag<sup>2+</sup> was present which was overcome by ion selective electrode.



In this research study, we conducted a comprehensive analysis of contaminant concentrations measured in Parts Per Million (PPM) in various villages situated within the Kalanaur block. Our findings reveal a wide range of PPM levels across the surveyed villages, reflecting the diversity of environmental conditions in this region. Among the villages studied, Nigana exhibited the highest contaminant concentration, recording a value of 0.009 PPM. Notably, Ballab and Marodi Jatan also had relatively high contamination levels at 0.005 PPM. Conversely, Kakrana displayed the lowest contaminant concentration, with a minimal 0.001 PPM. The remaining villages, including Anwal, Baniyani, Bhalli Anandpur, Garhi Ballab, Garnawathi, Gudan, Zindran, Kahnaur, Katesra, Kherdi, Lahli, Marodi Rangran, Patwarpur, Saimpal, Sanghera, Sundana, Taimurpur, Kalanaur, Kalanaur Kalan, and Majha, showed varying degrees of contaminant presence, with PPM levels ranging from 0.002 to 0.004. These findings underscore the heterogeneity of contaminant distribution in the Kalanaur region and emphasize the importance of further investigation and potential mitigation efforts to address environmental and public health concerns associated with these varying contamination levels.

### CONCLUSION

The urease enzyme was immobilised on a PTFE membrane and connected to an ammonium ion selective electrode (AISE) to form a biosensor. With

particle sizes ranging from 0.09  $\mu$ m to 0.49  $\mu$ m in diameter, the enzyme electrode was characterised using FTIR (Fourier transform infrared spectroscopy) and FESEM (Field emission scanning electron microscopy) techniques. The biosensor responded at its best within 20s when placed in a pH 5.5, 0.05mM urea conc., sodium phosphate buffer, and 40 °C environment. With a 38 mV/decade excellent sensitivity, a 0.001mM lower detection limit, and a larger linear range of 0.001 to 0.80mM, it demonstrated great performance. Analysis of the additional urea revealed that the following percentages were recovered: 99.6%, 101.08%, 107.4%, 100.4%, 97%, 71.37%, 99.06%, 102.3%, 100.2%, and 102.02%. In conclusion, a wide range of concentrations have been shown by the thorough analysis of the ammonia levels in the studied communities. This variety emphasises the necessity of ongoing monitoring and preventative actions in managing water quality throughout these locations.

In this research, we conducted an analysis of contaminant concentrations in several villages within the Kalanaur block, measured in Parts per Million (PPM). The findings reveal significant variations in PPM levels across the surveyed villages. Notably, Ballab and Basana exhibited higher contamination levels at 0.005 PPM, while Nigana had the highest PPM concentration at 0.009. Conversely, villages like Kakrana had lower contamination levels, recording only 0.001 PPM. These results indicate a diverse range of contaminant concentrations in different villages,

which may have important implications for environmental and public health considerations in the Kalanaur region.

## REFERENCES

- Antil, R.S., Narwal, R.P. and Gupta, A.P.1992. Urease activity and urea hydrolysis in soils treated with sewage. *Ecological Engineering*. 1(3): 229-237, (Elsevier).
- Chauhan, S. and Thakur, A. 2023. Chitosan-Based Biosensors-A Comprehensive Review. *Materials Today: Proceedings*, ISSN 2214-7853. <https://doi.org/10.1016/j.matpr.2023.01.123>.
- Chen, Z., Wang, Q., Zou, J.M.P. and Jiang, L. 2020. Impact of controlled-release urea on rice yield, nitrogen use efficiency and soil fertility in a single rice cropping system. *Sci. Rep.* 10: 10432. doi: 10.1038/s41598-020-67110-6 PubMed Abstract
- Choosang, J., Numnuam, A. and Thavarungkul, P. 2018. Simultaneous Detection of Ammonium and Nitrate in Environmental Samples Using an Ion-Selective Electrode and Comparison with Portable Colorimetric Assays. Published on October 19, 2018. Received on September 4, 2018, and Accepted on October 4, 2018.
- Cuartero, Mar, Colozza, Noemi, Fernández-Páez, Bibiana M. and Crespo, Gastón A. 2020. Why ammonium detection is particularly challenging but insightful with ionophore-based potentiometric sensors- an overview of the progress in the last 20 years. *The Analyst*. 145(9): 3188-3210. doi:10.1039/d0an00327a.
- Dhawan, G., Sumana, G. and Malhotra, B.D. 2009. Recent developments in urea biosensors. *Biochemical Engineering Journal*. 44(1): 42–52. doi:10.1016/j.bej.2008.07.004
- Getachew Woldemariam, Ali Kyad, Stephanie Moore, Jinshu Qiu, David Semin, Zhixin J. Tan and Jette Wypych, 2020. *PDA Journal of Pharmaceutical Science and Technology*. 74 (1): 2-1.
- Hamimed, S., Mahjoubi, Y., Abdeljelil, N., Gamraoui, A., Othmani, A., Barhoum, A. and Chatti, A. 2023. Chapter 18 - Chemical sensors and biosensors for soil analysis: principles, challenges, and emerging applications. In: A. Barhoum & Z. Altintas (Eds.), *Advanced Sensor Technology* (pp. 669-698). Elsevier. ISBN 9780323902229. <https://doi.org/10.1016/B978-0-323-90222-9.00014-5>.
- Jakhar, Seema and Pundir, C.S. 2017. Preparation, characterization and application of urease nanoparticles for construction of an improved potentiometric urea biosensors. *Biosensors and Bioelectronics*. S0956566317306115-. doi:10.1016/j.bios.2017.09.005
- Jiawang Ding and Wei Qin, 2020. Recent advances in potentiometric biosensors. *TrAC Trends in Analytical Chemistry*. 124:115803, ISSN 0165-9936, <https://doi.org/10.1016/j.trac.2019.115803>.
- Kira, O., Shaviv, A. and Dubowski, Y. 2019. Direct tracing of NH<sub>3</sub> and N<sub>2</sub> emissions associated with urea fertilization approaches, using static incubation cells. *Sci. Total Environ.* 661, 75–85. [PubMed]
- Lv, J., Zhang, X., Sha, Z., Li, S., Chen, X., Chen, Y. and Liu, X. 2024. Mitigation of reactive nitrogen loss from arable soils through microbial inoculant application: A meta-analysis. *Soil and Tillage Research*. 235: 105883. ISSN 0167-1987. <https://doi.org/10.1016/j.still.2023.105883>.
- Lambert, David, Sherwood, John and Francis, Paul, 2004. The determination of urea in soil extracts and related samples - A review. *Australian Journal of Soil Research - Aust J Soil Res*. 42: 10.1071/SR04028
- Pundir, C.S., Jakhar, Seema, Narwal, Vinay, 2018. Determination of urea with special emphasis on biosensors: A Review. *Biosensors and Bioelectronics*. S0956566318307668-. doi:10.1016/j.bios.2018.09.067.
- Raymond Vanholder, 2018. Urea and chronic kidney disease: the comeback of the century? (in uraemia research). *Nephrology Dialysis Transplantation*. 33(1): 4–12, <https://doi.org/10.1093/ndt/gfx039>
- Svane, S., Sigurdarson, J.J. and Finkenwirth, F. 2020. Inhibition of urease activity by different compounds provides insight into the modulation and association of bacterial nickel import and ureolysis. *Sci Rep.* 10: 8503. <https://doi.org/10.1038/s41598-020-65107-9>.
- United Nations Department of Economic and Social Affairs, Population Division, Global Population Growth and Sustainable Development. 2021. UN DESA/POP/2021/TR/NO.2.
- Wei, X., Chen, J., Gao, B. and Wang, Z. 2020. Role of controlled and slow release fertilizers in fruit crop nutrition. In: *Diagnosis and Management of Nutrient Constraints*, eds A. K. Srivastava and C. Hu (Amsterdam: Elsevier), 555–566. doi: 10.1016/B978-0-12-818732-6.00039-3. Google Scholar
- Wei, L.F. and Shih, J.S. 2001. Fullerene-cryptand coated piezoelectric crystal urea sensor based on urease. *Analytica Chimica Acta*. 437(1): 77–85. doi:10.1016/S0003-2670(01)00941-2
- Zhu, S., Liu, L., Xu, Y., Yang, Y. and Shi, R. 2020. Application of controlled release urea improved grain yield and nitrogen use efficiency: a meta-analysis. *Plos One*. 15: e0241481. doi: 10.1371/journal.pone.0241481 Google Scholar
- Zheng-Jiang Feng, Wei-Bo Nie, Yun-Peng Ma, Yu-chen Li, Xiao-Yi Ma, 2023. Hong-Yan Zhu, Effects of urea solution concentration on soil hydraulic properties and water infiltration capacity *Science of The Total Environment*, (Elsevier).